Collisional deactivation of highly vibrationally excited pyrazine

Laurie A. Miller
Department of Chemistry, University of Michigan, Ann Arbor, Michigan 48109-2143

John R. Barker[a)]
Department of Chemistry and Department of Atmospheric, Oceanic, and Space Sciences, University of Michigan, Ann Arbor, Michigan 48109-2143

(Received 18 March 1996; accepted 18 April 1996)

The collisional deactivation of vibrationally excited pyrazine ($C_4N_2H_4$) in the electronic ground state by 19 collider gases was studied using the time-resolved infrared fluorescence (IRF) technique. The pyrazine was photoexcited with a 308 nm laser and its vibrational deactivation was monitored following rapid radiationless transitions to produce vibrationally excited molecules in the electronic ground state. The IRF data were analyzed by a simple approximate inversion method, as well as with full collisional master equation simulations. The average energies transferred in deactivating collisions ($\langle \Delta E \rangle_d$) exhibit a near-linear dependence on vibrational energy at lower energies and less dependence at higher energies. The deactivation of ground state pyrazine was found to be similar to that of ground state benzene [J. R. Barker and B. M. Toselli, Int. Rev. Phys. Chem. **12**, 305 (1990)], but it is strikingly different from the deactivation of triplet state pyrazine [T. J. Bevilacqua and R. B. Weisman, J. Chem. Phys. **98**, 6316 (1993)]. [S0021-9606(96)01228-7]

I. INTRODUCTION

Pyrazine has been used extensively in studies of collision-free energy redistribution[1] and its photophysics are very well known.[2–5] Several groups have studied its collisional deactivation subsequent to photoexcitation. McDonald and Rice investigated collisional energy transfer among low energy vibrational states in the first excited singlet state.[6] Mullin, Flynn, and co-workers used time-resolved tunable diode laser spectroscopy to investigate energy transfer from vibrationally excited ground state pyrazine (vibrational energy $E=40\,640$ cm^{-1}) to the asymmetric stretch of CO_2 after a single collision.[7–9] They observed energy transfer to the vibrational, rotational, and translational degrees of freedom of the CO_2, but only the first collision was probed, and they reported no information regarding the succeeding collisions and the population distribution of the excited molecules.

Bevilacqua and Weisman[3] studied the energy loss from vibrationally excited triplet state pyrazine by measuring the rate of intersystem crossing (ISC) from triplet to singlet, which is a function of the triplet state vibrational energy.[2–4] Their results indicated that $\langle\langle \Delta E \rangle\rangle$, the average energy transferred per collision rises from an apparent threshold which lies between 2000 and 3000 cm^{-1} and is strongly energy dependent between 3000 and 5000 cm^{-1}. This steep energy dependence and sudden threshold are in sharp contrast to the linear or less than linear energy dependence observed for other molecules in the electronic ground state.[10–12]

The present work was motivated by a desire to determine the energy transfer properties of pyrazine in the ground electronic state and to compare them with the results of Flynn and co-workers and Bevilacqua and Weisman. Experiments on the temperature dependence of pyrazine energy transfer parameters will be described elsewhere.[13] The present study of pyrazine is one of a class of large molecule energy transfer studies performed using physical techniques, as distinguished from unimolecular reaction studies.[14] Physical energy transfer techniques which rely on radiationless transitions include ultraviolet absorption,[15] multiple photon ionization,[16] diode laser absorption spectroscopy,[17] and infrared fluorescence (IRF). Methods which use CO_2 laser pumping in the electronic ground state include time resolved optoacoustic and mercury tracer techniques.[10] A number of benzene and toluene isotopomers have been investigated using single-color IRF and several have been investigated using multicolor IRF, which provides more detailed information about the population distribution of excited molecules.[18–25] Pyrazine is a diazo-substituted benzene with 10 atoms and 24 vibrational modes: A size slightly smaller than the 12 atoms and 30 vibrational modes found in benzene, with which it can be compared.

In the present study, pyrazine is excited to the first singlet state via a 308 nm laser pulse. Rapid intersystem crossing (ISC) occurs to the first triplet state.[1] On a slightly slower time scale ($\tau \approx 0.2\ \mu s^2$), the molecule crosses by ISC to the ground state singlet manifold to produce ground electronic state pyrazine with $\sim 32\,500$ cm^{-1} of vibrational energy. As the vibrationally excited molecules are collisionally deactivated, IRF from the C–H stretch is monitored. The intensity of IRF depends on the average vibrational energy of the excited population through a well tested theoretical expression,[18,26,27] which is used to deduce energy loss as a function of vibrational energy. Master equation simulations are used to simulate the experiments and to deduce $\langle \Delta E \rangle_d$, the average energy transferred in each deactivating collision.

[a)]Address correspondence to this author. Electronic mail: jrbarker@umich.edu

II. EXPERIMENT

The IRF technique has been described in detail elsewhere.[18,19] Gas phase pyrazine in a 2.5 cm diameter by 30 cm long glass cell with fused silica end windows was irradiated by a XeCl excimer laser (308 nm) operating at a pulse repetition frequency of 25 Hz. Direct absorption measurements in our laser apparatus gave an absorption cross section of $\sim 1.33 \pm 0.03 \times 10^{-18}$ cm^2 (base e) at the laser wavelength (308 nm). This value is consistent with the cross section of $\sim 1.4 \times 10^{-18}$ cm^2 found from the highly detailed absorbance spectrum in Ref. 23. Typical laser fluences were ~ 12 mJ cm^{-2} and thus only about 0.5% of the irradiated pyrazine was excited in each laser shot. Infrared emission from the C–H stretch near 3030 cm^{-1} was monitored through sapphire side windows with an InSb photovoltaic detector (Infrared Associates) equipped with a matched preamplifier. The signal was further amplified with a Tektronix AM-502 preamplifier and recorded on a LeCroy 9400 digital oscilloscope. The time response of the detection system was ~ 3 μs. Approximately 8000 laser shots were averaged for each run, and the data were transferred from the digital oscilloscope to a Macintosh computer for storage and analysis.

The IRF technique for measuring energy transfer breaks down at very high and very low pressures. In the limit of low pressure, the excited molecules relax primarily through IRF emission, instead of collisions.[20,28,29] At very high pressures, the assumption of bimolecular collisions breaks down. Experimental limitations further restrain the range of applicable pressures. The IRF signal is attenuated at low pressure by diffusion from the field of view of the detector and at high pressure by reabsorption of the IRF by surrounding molecules. The pressure range used in the present experiments avoids these potential difficulties.

In the present work, the experiments were performed using flowing conditions in order to minimize any potential accumulation of photodissociation products. A capacitance manometer (MKS Baratron, 0–10 Torr) was used to measure the pressure in the cell. For pyrazine-only studies, the pressure ranged from 20 to 90 mTorr. Below 20 mTorr, diffusion from the field of view of the detector was observed to affect the IRF decay data. For the experiments which used added collider gases, the pressure of pyrazine was held constant at around 8 mTorr and the collider gas pressure was varied from $\sim$50 mTorr up to as high as 300 mTorr. In a few experiments with CO_2 collider, spontaneous IRF from the CO_2 asymmetric stretch mode was observed with a 4 μm long-pass filter, but quantitative experiments were not performed.

At the relatively low pressures of pyrazine used in the collider gas experiments, IRF emission at ~ 6000 cm^{-1} from the C–H stretch overtone was too weak to be quantified. Only the fundamental band intensity decays were used in the analysis that follows. In the temperature dependent pyrazine IRF studies to be described elsewhere,[13] both bands are analyzed in order to gain more information about the population distribution of the excited species.[20,29]

Pyrazine is known to photodissociate at short wavelengths, but the quantum yield is negligible at 308 nm. Chesko *et al.*[5] estimate the quantum yield for HCN production to be $\phi \approx 0.003$ under collision-free conditions. The issue has been raised that the pyrazine photodissociation at 248 nm may produce a significant yield of HCN ($\phi \approx 0.40$) which can recoil and perhaps produce the excited CO_2 states detected by Flynn and co-workers.[5] Flynn and co-workers[30] responded to this suggestion by pointing out that the extent of dissociation is small at the 1 μs time delay used in their experiments and the collisional deactivation slows the decomposition rate even more. They carried out experiments which support this assertion and concluded that their energy transfer results are not affected significantly.[30] At 308 nm, the collision free photodissociation yields are 100 times smaller and no pressure increases or window deposits were observed in the present experiments. Even if photodissociation products were present, they would have very little residual vibrational energy and would not contribute significantly to the IRF.

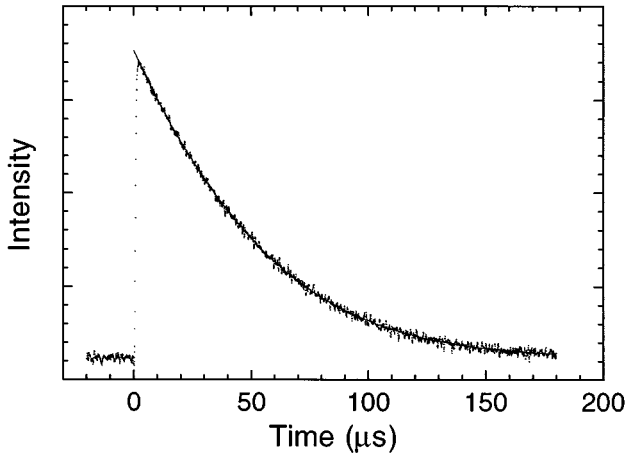

FIG. 1. Experimental IRF signal from excited pyrazine deactivation by unexcited pyrazine. Line is least squares fit to the data, and extrapolated to $t=0$.

Pyrazine (Sigma 99%) was degassed in several freeze–pump–thaw cycles (77 K) before use. The collider gases were obtained from Cryogenic Rare Gas (neon 99.999%, krypton 99.999%, xenon 99.999%), Liquid Carbonic (helium 99.999%, argon 99.999%, nitrogen 99.999%, oxygen 99.995%, nitric oxide 99%), Matheson (deuterium), Air Products (hydrogen 99.9995%), BOC (carbon dioxide 99.999%), and C.P. grade from various sources: carbon monoxide, ammonia, methane, propane, butane, sulfur hexafluoride). Nitric oxide, butane, and propane were further purified by bulb-to-bulb distillation.

III. RESULTS

A. Treatment of experimental data

An example of an infrared fluorescence decay curve is presented in Fig. 1. The data from the first ~ 3 μs were strongly affected by the detector rise time, so the IRF inten-

sity (which includes a time-independent contribution from the cell walls) was extrapolated to $t=0$ using the expression

$$I=A\ \exp(-k't-b't^2)+G, \tag{1}$$

where k' and b' are empirical parameters fitted by nonlinear least squares. The data are normalized by setting $A=1$ and $G=0$.

For convenience, the IRF decay curves were converted from a time scale to a collision scale according to the expression

$$Z=\omega t=(k^c_{\mathrm{LJ}}N_c+k^p_{\mathrm{LJ}}N_p)t, \tag{2}$$

where Z is the number of collisions, k^c_{LJ} and k^p_{LJ} are the Lennard-Jones bimolecular collision rate constants[3,31] for parent–collider and parent–parent interactions, respectively, and N_c and N_p are the number densities of collider and parent molecules, respectively. After converting to the collision scale, the IRF intensity can still be described by a function similar to Eq. (1) with t replaced by Z and with new parameters k and b expressed in units of Z^{-1} and Z^{-2}, respectively.

Each mixture of pyrazine and collider is characterized by a collision fraction which gives the average fraction of collisions experienced by a pyrazine molecule with the added collider gas

$$F_c=\frac{k^c_{\mathrm{LJ}}N_c}{k^c_{\mathrm{LJ}}N_c+k^p_{\mathrm{LJ}}N_p}. \tag{3}$$

To extrapolate the data to the limit of pure collider gas, the fitted parameters $k(F_c)$ and $b(F_c)$ from Eq. (1) for a particular experiment characterized by F_c are plotted as a function of F_c and least squares fitted with a quadratic equation. Figure 2 shows a typical F_c plot. Extrapolation to $F_c=1$ gives values of $k(F_c=1)$ and $b(F_c=1)$ corresponding to deactivation of pyrazine exclusively by the collider gas. The parameters $k(F_c=1)$ and $b(F_c=1)$ can be used with Eq. (1) to generate synthetic data sets corresponding to the $F_c=1$ limiting case.

B. Approximate data inversion

The theoretical expression relating the IRF intensity to bulk average energy has been described elsewhere.[18,26] In several experimental tests, the theoretical relationship has been shown to be accurate.[18,21,22,26,27] For pyrazine, the theoretical relationship was calculated using a vibrational assignment[32] and assuming that one rotational degree of freedom is active,[33] as summarized in Table I. For singlet state pyrazine, an empirical least squares fit of the vibrational energy E and the theoretically calculated C–H stretch band intensity I near 3030 cm^{-1} is

$$E=950+15011I+8651I^{0.5}+8176I^{0.25}, \tag{4}$$

where I has been normalized to unity at 32 500 cm^{-1}. This relationship is valid for the energy range from ~5000 to ~35 000 cm^{-1}.

As described elsewhere,[18,20,22,24] the bulk average energy $\langle\langle E(t)\rangle\rangle$ (averaged over the population distribution, which evolves with time) can be extracted approximately by using the time dependent observed intensity. To do this, the experimental intensity is identified with I (the calculated intensity) and the bulk average energy $\langle\langle E\rangle\rangle$ is identified with E in Eq. (4). To emphasize that this approximate technique has been used to invert the data, the subscript ''inv'' is appended: $\langle\langle E\rangle\rangle_{\mathrm{inv}}$. The derivative of $\langle\langle E\rangle\rangle_{\mathrm{inv}}$ with respect to Z gives $\langle\langle \Delta E\rangle\rangle_{\mathrm{inv}}$, the bulk average vibrational energy transferred by pyrazine per collision.

The parameters $k(F_0=1)$ and $b(F_0=1)$ were used with Eq. (1) to generate a synthetic data set and Eq. (4) was used to determine $\langle\langle E(Z)\rangle\rangle_{\mathrm{inv}}$ as a function of collisions. This curve was least squares fitted with a quadratic exponential function similar to Eq. (1) and the resulting parameters were used to compute the derivative with respect to Z. The resulting curves showing $\langle\langle \Delta E(E)\rangle\rangle_{\mathrm{inv}}$ as a function of $\langle\langle E\rangle\rangle_{\mathrm{inv}}$

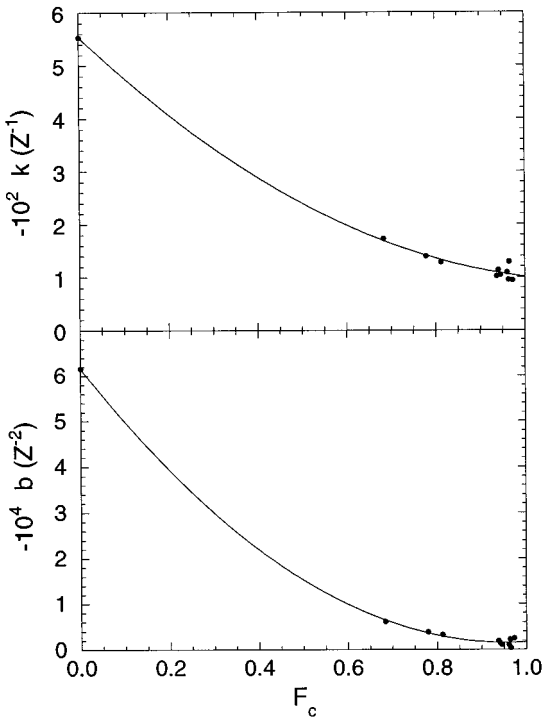

FIG. 2. Decay parameters $-k(Z^{-1})$ and $-b(Z^{-2})$ vs collision fraction F_c of CO_2.

TABLE I. Vibrational assignments and moments of inertia for pyrazine.

Pyrazine (S_0)
Active rotor moment of inertia: 80.47 amu Å (Ref. 33)
Harmonic oscillators (cm^{-1}) (Ref. 32) 3055, 1580, 1233, 1016, 602, 960, 350, 927,3012, 1483, 1130, 1018, 983, 756, 3069.06, 1411, 1149, 1063, 3040, 1525,1346, 704, 785, 418.

Pyrazine (T_1) (Ref. 3)
Active rotor moment of inertia: 80 amu $\mathrm{Å}^2$.
Harmonic oscillators (cm^{-1}): 980, 3055, 1346, 537, 522, 620, 624, 3040, 1230,1525, 1146, 440, 563, 1021, 3012, 1149, 406, 237, 743, 1136, 1063, 1484,1416, 3063.

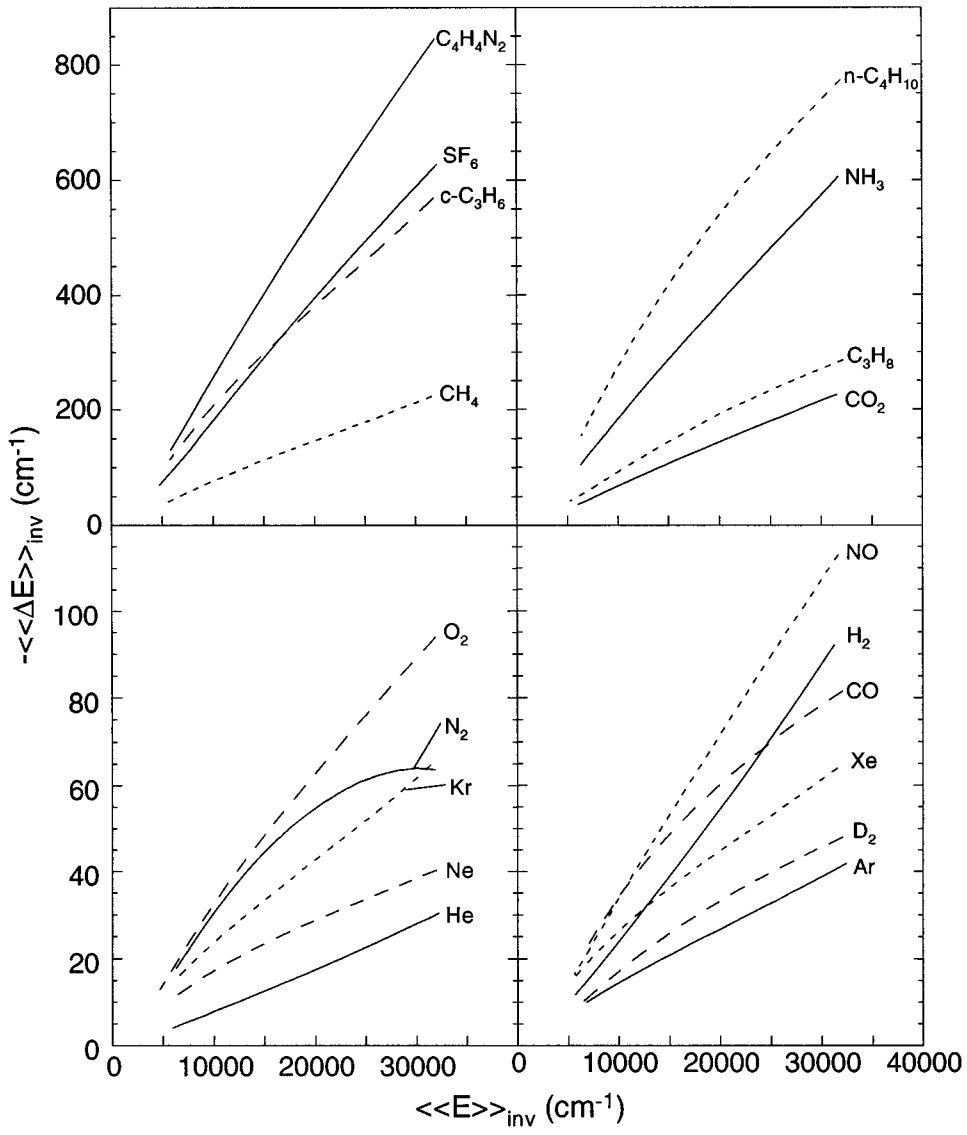

FIG. 3. $-\langle\langle \Delta E\rangle\rangle_{\text{inv}}$ vs $\langle\langle E\rangle\rangle_{\text{inv}}$ for excited pyrazine deactivated by various colliders.

are shown in Fig. 3, and values of $\langle\langle \Delta E(E)\rangle\rangle_{\text{inv}}$ at $\langle\langle E\rangle\rangle_{\text{inv}}=24\,000\ \text{cm}^{-1}$ are presented in Table II.

Upward, as well as downward energy transfer steps contribute to $\langle\langle \Delta E(E)\rangle\rangle_{\text{inv}}$. In order to extract $\langle \Delta E(E)\rangle_d$ the average step size for down steps, further analysis is necessary. The following expressions are based on the conventional exponential model and they can be used to least squares fit the data for $\langle\langle \Delta E\rangle\rangle_{\text{inv}}$ vs $\langle\langle E\rangle\rangle_{\text{inv}}$ and obtain an estimate for $\langle \Delta E(E)\rangle_d$:[27]

$$\langle\langle \Delta E(E)\rangle\rangle_{\text{inv}}=D^{-1}-\langle \Delta E(E)\rangle_d, \tag{5a}$$

$$D=\langle \Delta E(E)\rangle_d^{-1}+(k_BT)^{-1}-B, \tag{5b}$$

$$B=\frac{s-1+r/2}{E+a(E)E_z}, \tag{5c}$$

where k_B is the Boltzmann constant, s is the number of vibrational modes, r is the number of rotors, E_z is the zero point energy, and $a(E)$ is a parameter in the Whitten–Rabinovitch approximation.[34–36] The Whitten–Rabinovitch parameters for pyrazine are summarized in Table III. The data are accurately fitted if $\langle \Delta E(E)\rangle_d$ is assumed to have a quadratic energy dependence (higher order terms were not necessary in the fitting)

$$\langle \Delta E(E)\rangle_d=b_0+b_1E+b_2E^2. \tag{6}$$

The polynomial coefficients for each collider are listed in Table II. Propagation of the errors gives estimated uncertainties on the order of 2% to 5%. These errors describe only the goodness of fit of the theoretical expression, and do not account for any systematic errors inherent in the expression itself. The coefficients not only provide an estimate for $\langle \Delta E(E)\rangle_d$, but they can also be used with Eq. (5) to reproduce the data for $\langle\langle \Delta E\rangle\rangle_{\text{inv}}$ vs $\langle\langle E\rangle\rangle_{\text{inv}}$.

TABLE II. Collider gas data.

	Lennard-Jones Parameters[a]				$\langle\Delta E\rangle_d$[d]			$\alpha(E)$[e]		
	σ_{LJ} Å	ϵ/k (K)	$10^{10}\,k_{LJ}$ $cm^3\,s^{-1}$	$-\langle\langle\Delta E\rangle\rangle_{inv}$[b,c] cm^{-1}	b_0 cm^{-1}	$100\,b_1$	$10^7\,b_2$ $1/cm^{-1}$	C_0 cm^{-1}	$100\,C_1$	$10^7\,C_2$ $1/cm^{-1}$
$C_4H_4N_2$	5.35	436	6.59	657± 4	110	3.09	−0.658	100	3.05	−1.0
He	2.55	10.22	6.30	22± 4	16.6	0.365	−0.246	22.1	0.325	−0.31
Ne	2.82	32.8	3.84	33± 2	39.8	0.427	−0.483	43.4	0.389	−0.47
Ar	3.47	114	4.21	32± 4	34.5	0.388	−0.296	43	0.326	−0.32
Kr	3.66	178	3.84	51± 2	47.2	0.509	−0.359	49	0.482	−0.44
Xa	4.05	230	3.99	52± 4	50.2	0.553	−0.557	55	0.50	−0.60
H_2	2.83	60	12.0	67± 2	22.1	0.812	−0.567	30	0.72	−0.72
D_2	2.73	69	8.60	39± 1	27.2	0.606	−0.735	37	0.49	−0.655
N_2	3.74	82	4.80	60± 1	29.2	0.947	−1.61	37	0.915	−1.8
O_2	3.84	103	4.85	74± 2	36.0	0.845	−0.899	36	0.90	−1.5
CO	3.70	105	4.83	69± 3	46.6	0.79	−1.02	53	0.81	−1.45
NO	3.49	117	4.70	86±10	31.4	0.907	−0.770	40	0.89	−1.0
CO_2	3.94	201	5.02	173± 3	42.2	1.43	−1.08	54	1.25	−1.1
CH_4	3.79	153	6.74	174± 7	67.0	1.3	−0.991	88	1.10	−1.21
NH_3	2.90	558	7.01	461±10	60.7	2.91	−1.74	78	2.74	−1.9
SF_6	5.20	212	4.85	476±22	40.6	3.17	−2.10	56	2.90	−2.4
C_3H_8	4.78	271	6.33	226± 4	40.5	1.92	−1.94	76	1.60	−1.8
c-C_3H_6	4.63	299	6.37	449±20	108	2.72	−2.03	130	2.50	−2.0
n-C_4H_{10}	5.40	307	6.72	627±22	49.1	4.36	−4.55	55	4.70	−7.5

[a]Lennard-Jones parameters for collider gases from Ref. 30; for pyrazine, from Ref. 3.
[b]Uncertainties are $\pm 2\sigma$ statistical errors.
[c]Evaluated at $\langle\langle E\rangle\rangle_{inv}=24\,000\ cm^{-1}$.
[d]$\langle\Delta E(E)\rangle_d=b_0+b_1E+b_2E^2$; coefficients are least squares fit to the theoretical expression.
[e]$\alpha(E)=C_0+C_1E+C_2E^2$; coefficients are ''optimized'' using master equation simulations.

C. Master equation simulations

The energy transfer data can be analyzed without the need for approximate inversions. This is accomplished by using an empirical step-size distribution function and numerical solution of the collisional master equation to obtain calculated IRF intensities for comparison with the experimental data. This approach has not been ''automated'' and the simulations require some judgment. The stochastic master equation formulation used in the present work has been described in detail elsewhere.[37,38] Basically, it employs an empirical step size model and Monte Carlo techniques to select the initial conditions and the progress of each stochastic trial, based on microscopic reversibility and detailed balance. In this work, the exponential model was used for the collision step-size distribution, which describes the probability of a transition from energy E to energy E'. The functional form for the exponential model for down steps is given by

$$P(E',E)=M(E)\exp[-(E-E')/\alpha(E)], \quad E'<E, \quad (7)$$

where $\alpha(E)$ is an energy-dependent parameter which is almost identical to $\langle\Delta E(E)\rangle_d$ and $M(E)$ is the normalization constant, which depends on energy. The master equation simulation computer code uses the theoretical expression for the energy-dependent microcanonical IRF emission intensity to calculate the bulk average IRF intensity, which is compared directly with the experimental results. By adjusting the parameters in the collisional energy transfer model, it is possible to achieve nearly exact agreement between simulation and experiment.

In practice, the master equation simulations were carried out using the fitted expression for $\langle\Delta E(E)\rangle_d$ [Eq. (6)] as an initial estimate for $\alpha(E)$, which was assumed to have the functional form

$$\alpha(E)=C_0+C_1E+C_2E^2. \quad (8)$$

For comparisons between the simulations and the experiments, the calculated IRF curves were inverted to energy profiles and $\langle\langle\Delta E\rangle\rangle_{inv}$ vs $\langle\langle E\rangle\rangle_{inv}$ data sets were generated in exactly the same way described above for the experimental data. The master equation simulations which used the initial estimates for $\alpha(E)$ agreed with the experimental data to within 10% to 25%, as shown in Fig. 4. In order to optimize the simulations, the parameters C_0, C_1, and C_2 were ad-

TABLE III. Whitten–Rabinovitch parameters[a] for pyrazine.

	Pyrazine (S_0)	Pyrazine (T_1)
Active rotor[b]	1	1
Harmonic oscillators[c]	24	24
Zero-point energy	16 307 cm^{-1}	15 179 cm^{-1}
Geometric mean frequency	1156.8 cm^{-1}	1013.8 cm^{-1}
β	1.3037	1.4410

[a]For definitions and notation, see Refs. 34, 35, and 36.
[b]Pyrazine (S_0) assignment and moments of inertia from Ref. 33; pyrazine (T_1) assignment estimated based on singlet geometry; see Table I.
[c]Singlet assignment from Ref. 32; triplet assignment from Ref. 3; see Table I.

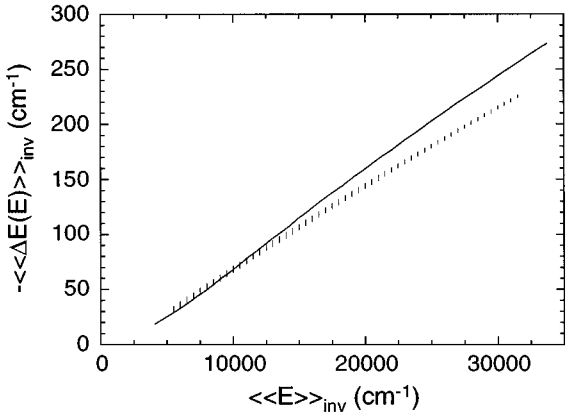

FIG. 4. Master equation simulations (solid line) compared with experimental results ($\pm 1\sigma$ error bars) for $-\langle\langle \Delta E\rangle\rangle_{\text{inv}}$ vs $\langle\langle E\rangle\rangle_{\text{inv}}$ for pyrazine deactivated by CO_2. The $\alpha(E)$ parameters for the simulation are those determined for $\langle \Delta E\rangle_d$, as described in the text.

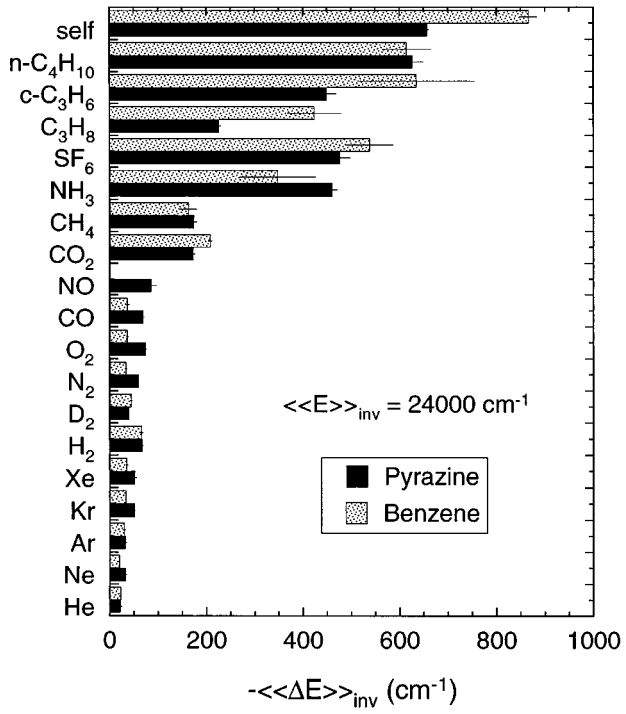

FIG. 5. Magnitudes of $-\langle\langle \Delta E\rangle\rangle_{\text{inv}}$ for deactivation of excited benzene (Ref. 18) and excited pyrazine (this work) evaluated at $\langle\langle E\rangle\rangle_{\text{inv}}=24\,000\ \text{cm}^{-1}$. Error bars are $\pm 2\sigma$.

justed to give better agreement with the experimental data. Table II lists the optimized parameters for each collider. These ''optimized'' parameters when used with the master equation provide an accurate description of the experimental data. Because the optimized parameters are determined on the basis of judgment, it is difficult to propagate statistical errors, but we estimate the optimized simulations to be accurate to better than $\pm 5\%$ over the energy range from $\sim 5\,000$ to $\sim 33\,000\ \text{cm}^{-1}$.

IV. DISCUSSION

A. Comparison with benzene

The collisional vibrational energy loss of pyrazine is similar to that of benzene.[18] The energy dependence of $\alpha(E)$ is quite important in unimolecular reactions.[38,39] As in benzene and the other benzene and toluene isotopomers, the energy dependence of $\alpha(E)$ for pyrazine is approximately linear. In Fig. 5, $\langle\langle \Delta E(E)\rangle\rangle_{\text{inv}}$ values for pyrazine and benzene evaluated at $\langle\langle E\rangle\rangle_{\text{inv}}=24\,000\ \text{cm}^{-1}$ are presented for the various collision partners. For both excited species, the energy transferred per collision tends to increase with the increasing complexity of the collider. For monatomic and diatomic colliders, the $\langle\langle \Delta E(E)\rangle\rangle_{\text{inv}}$ values for pyrazine are slightly greater than those for benzene, but for the polyatomic colliders (except for ammonia) the values tend to be somewhat smaller. The similarity between pyrazine and benzene is likely due to the comparable molecular structure, density of states, and vibrational frequencies.

This is the first time that nitric oxide has been used as a collider in IRF studies and the energy transfer results are quite similar to CO, N_2, and O_2 collider gases. There were no indications of chemical reaction or other complications in the experiments using nitric oxide.

Although classical trajectory calculations on large molecule energy transfer suffer from several problems,[40–42] recent calculations provide some insight into the qualitative features of energy transfer, and these same features are probably operative in the deactivation of pyrazine. First, in $V-T/R$ energy transfer, direct impulsive collisions and ''chattering'' collisions are far more important than complex formation in which statistical energy transfer occurs.[41,43–45] Second, $V-V$ energy transfer appears to dominate in benzene self-deactivation collisions.[46] The present results for pyrazine are consistent with the trajectory calculations, but they cannot distinguish among the mechanisms of energy transfer.

B. Comparison with pyrazine (T_1)

Bevilacqua and Weisman[3] determined the bulk average energy transfer step size $\langle\langle \Delta E(E)\rangle\rangle$ for triplet state pyrazine deactivation by several colliders. Their results extend from near the triplet origin up to about 5000 cm^{-1} above the origin. The present data for the electronic ground state extend down only to about 5000 cm^{-1}, because at lower vibrational energies the IRF intensities become too low for reliable measurements. Data for both triplet and singlet pyrazine deactivation by several colliders are summarized in Table 4 for a vibrational energy of $\langle\langle E\rangle\rangle=5000\ \text{cm}^{-1}$. At 5000 cm^{-1}, the singlet state values for $\langle\langle \Delta E\rangle\rangle$ are much smaller than those for triplet pyrazine. In addition, the triplet experiments found that $\langle\langle \Delta E(E)\rangle\rangle$ is nearly zero below 2000 cm^{-1} and then increases steeply with energy between 2000 and 5000 cm^{-1}. The data for singlet pyrazine do not show this effect, but they are only reliable for energies greater than 5000 cm^{-1}.

In order to further compare our results to those of Bevilacqua and Weisman, we carried out master equation simulations of their experiments. For pyrazine (T_1), we employed the S_0 electronic state Lennard-Jones parameters listed in

TABLE IV. Comparison of energy loss per collision.

Collider	$-\langle\langle\Delta E\rangle\rangle$[a] ($cm^{-1}$) at $\langle\langle E\rangle\rangle = 5000$ cm^{-1}	
	Pyrazine (S_0)[b,c]	Pyrazine (T_1)[d]
He	3±16	51
Ar	7± 4	142
H_2	10± 2	99
SF_6	78±96	433
Pyrazine	113± 2	316

[a]$\langle\langle E\rangle\rangle$ and $\langle\langle\Delta E\rangle\rangle$ from different data inversions in the two studies.
[b]This work.
[c]Uncertainties are $\pm 2\sigma$ statistical errors.
[d]From Ref. 3.

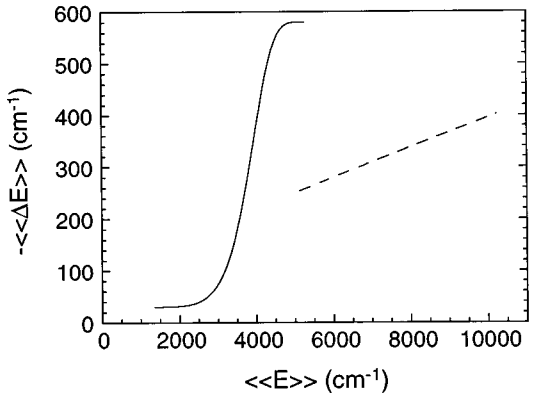

FIG. 6. Values of $\alpha_t(E)$ for pyrazine (T_1) (solid line) and $\alpha(E)$ for pyrazine (S_0) (broken line) determined using master equation simulations.

Table II, but we used a T_1 state vibrational assignment[3] in calculating densities of states. Bevilacqua and Weisman describe a calibration curve which relates the $T_1 \rightarrow S_0$ ISC rate to the average vibrational energy in the T_1 state. We incorporated ISC in the master equation calculations by treating it as a unimolecular process with microcanonical rate constants defined by the Bevilacqua and Weisman calibration curve.

At low pressures, most of the excited T_1 molecules decay via ISC prior to collisional deactivation within the T_1 state, but at high pressures, most T_1 molecules experience collisional deactivation prior to undergoing ISC. We found that the strong energy dependence and threshold of $\langle\langle\Delta E(E)\rangle\rangle$ observed experimentally can be simulated with a conventional exponential model characterized by a special energy-dependent parameter $\alpha_t(E)$. In the ground electronic state, the corresponding parameter $\alpha(E)$ is approximately linearly dependent on energy and is accurately described by a quadratic energy dependence from 5000 to 35 000 cm^{-1}. This quadratic energy dependence is totally inadequate for describing the triplet state, however. Instead, the following (nonunique) empirical function was found to produce results in good agreement with the Bevilacqua and Weisman experiments:

$$\alpha_t(E) = A(1 - \exp(-[E/\gamma]^c)) + D. \tag{9}$$

The exponential function was chosen because it accurately models the steep energy dependence, but other empirical functions may work just as well.

Optimum values for the empirical parameters in Eq. (9) were found by trial and error (see Table V) and they are similar to the results deduced by Bevilacqua and Weisman.[3] ''Optimized'' $\alpha_t(E)$ and $\alpha(E)$ functions for the deactivation of triplet and of singlet state pyrazine, respectively, by unexcited pyrazine are presented in Fig. 6. For singlet state pyrazine, the IRF technique is not reliable below about 5000 cm^{-1} and it is not known whether $\alpha(E)$ exhibits threshold behavior at lower energies. The magnitudes of the energy transfer parameters depend strikingly on the character of the electronic state, although the vibrational densities of states are similar. Bevilacqua and Weisman have offered some ideas regarding this difference, but it is fair to say that the reasons for the difference are not yet understood.

TABLE V. $\alpha_t(E)$ Parameters for pyrazine (T_1).[a]

Parameter	Optimized values[b]
A (cm^{-1})	500
γ (cm^{-1})	4000
c	8.7
D (cm^{-1})	30

[a]Optimized master equation fit of experimental data from Ref. 3.
[b]$\alpha_t(E) = A\ \{1 - \exp(-[E/\gamma]^c)\} + D$.

The triplet state modeling enables us to address a possible complication in the IRF experiments. At collision frequencies greater than $\sim 10^6$ s^{-1}, collisions occur before completion of the radiationless transitions to the electronic ground state. If significant vibrational deactivation occurs in the triplet state, IRF from the ''trapped'' species is either lost or delayed by the slower ISC rate. Collisional deactivation is faster in the triplet state than in the singlet state, but the rapidly cascading triplet population will be delayed by the slow ISC rate near the triplet state origin. In the monatomic collider experiments, in which pressures up to 300 mTorr were used, the collision rate becomes comparable to the ISC rate. Master equation simulations show that in the helium system at the highest collision frequencies employed in any of the present experiments, ~75% of the excited population undergoes ISC before one Lennard-Jones collision occurs. The remaining triplet state molecules complete the radiationless transition within 1 μs (compared to the 3 μs rise time of the detector) so IRF in the singlet state should be visible for all excited molecules. The effect of the ~25% of the triplet population which do experience a collision before ISC would be to alter the distribution of excited species being deactivated in the electronic ground state. However, the monatomic colliders only weakly deactivate triplet state pyrazine,[3] so we expect the distortion of the population distribution to be small. The experimental data at high collision frequencies are indistinguishable from those obtained at much lower pressures, and we conclude that the effect of triplet state collisional deactivation is negligible.

C. Comparison with pyrazine+CO_2 product probe studies

Mullin, Flynn, and co-workers[7–9] probed the CO_2 collider bath following one collision with vibrationally excited pyrazine, and found the amount of energy transferred to rotations and translations in $CO_2(00°0)$ and in $CO_2(00°1)$. They found that the deactivation of pyrazine appears to be dominated by $V-T/R$ energy transfer. By using an approximate model,[9] they estimated that $\geqslant 400$ cm^{-1} is transferred per collision to the $J=58-82$ rotational states of the CO_2 collider from pyrazine excited to $\sim 40\,640$ cm^{-1}. This estimate can be compared with the present IRF experimental results extrapolated to the higher energy: $\langle \Delta E \rangle_d = \alpha(40\,640) \approx 380 \pm 60$ cm^{-1} and $\langle \Delta E(40\,640) \rangle_{\text{all}} = -275 \pm 30$ cm^{-1}. The agreement is not satisfactory, when one considers the fact that the Mullin, Flynn, and co-workers estimate refers only to production of a limited subset of CO_2 rotational levels; if the other rotational levels were included, their estimate would likely be much higher.

In a key part of their analysis, Mullin *et al.*[9] took their measured rate constants k^I for the production of $CO_2(00°0,J)$ in each of seven rotational states between $J=58$ and $J=82$, and used them with an *ad hoc* heuristic model. In the model, they assumed that the cross sections follow an energy-gap law for both the translational energy changes and the angular momentum changes. Because the internal states of pyrazine were not observable in their experiments, they did not consider them explicitly. The pyrazine vibrational state densities are necessary to maintain microscopic reversibility and their omission may explain the difference between the Mullin *et al.* estimates and the energy transfer parameters determined in the present work. A detailed comparison of the two experiments is not straightforward, but it should be undertaken in future work.

V. CONCLUSIONS

Vibrational energy transfer from highly excited pyrazine to various colliders was studied using the IRF technique. The average energy transferred per collision is approximately proportional to energy between 5000 and 25 000 cm^{-1}, and it often tends to level off at higher energies. The magnitude of the energy transferred per collision depends on the complexity of the collider, as expected from phenomenological trends observed for other gas phase aromatic molecules.[15,18,19,12,20,21,22,24,27,47]

Collisional energy transfer in the pyrazine singlet state (this work) and triplet state[3] have distinctly different magnitudes and energy dependencies. Master equation simulations were performed for both singlet and triplet state data. Energy transfer from both electronic states is energy dependent, but triplet energy transfer is much more efficient and exhibits a sharp threshold between 2000 and 3000 cm^{-1}.

In experiments carried out using CO_2 collider, values for $\langle\langle \Delta E \rangle\rangle$ and $\langle \Delta E \rangle_d$ were obtained, but the results cannot be compared with those obtained by tunable diode laser monitoring of CO_2 internal states, because of the way the tunable diode laser data were analyzed. Future work should address analysis methods which will enable comparisons between the different experiments.

ACKNOWLEDGMENTS

Thanks go to the Office of Basic Energy Sciences at the U.S. Department of Energy for funding. Thanks also go to Jerrell D. Brenner and to Ralph E. Weston, Jr. for helpful discussions, and to George W. Flynn for discussions and for communicating results to us prior to publication.

[1] J. Kommandeur, W. A. Majewski, W. L. Meerts, and D. W. Pratt, Ann. Rev. Phys. Chem. **38**, 433 (1987).
[2] J. Knee and P. Johnson, J. Phys. Chem. **89**, 948 (1985).
[3] T. J. Bevilacqua and R. B. Weisman, J. Chem. Phys. **98**, 6316 (1993).
[4] O. Sneh, D. Dünn-Kittenplon, and O. J. Cheshnovsky, Chem. Phys. **91**, 7331 (1989).
[5] J. D. Chesko, D. Stranges, A. G. Suits, and Y. T. Lee, J. Chem. Phys. **103**, 6290 (1995).
[6] D. B. McDonald and S. A. Rice, J. Chem. Phys. **74**, 4709 (1981).
[7] A. S. Mullin, C. A. Michaels, and G. W. Flynn, J. Chem. Phys. **102**, 6032 (1995).
[8] A. S. Mullin, J. Park, J. Z. Chou, G. W. Flynn, and R. E. Weston, Jr., Chem. Phys. **175**, 53 (1993).
[9] C. A. Michaels, A. S. Mullin, and G. W. Flynn, J. Chem. Phys. **102**, 6682 (1995).
[10] I. Oref and D. C. Tardy, Chem. Rev. **90**, 1407 (1990).
[11] M. Damm, H. Hippler, and J. Troe, J. Chem. Phys. **88**, 3564 (1988).
[12] J. Shi and J. R. Barker, J. Chem. Phys. **88**, 6219 (1988).
[13] C. D. Cook, L. A. Miller, and J. R. Barker (unpublished).
[14] D. C. Tardy and B. S. Rabinovitch, Chem. Rev. **77**, 369 (1977).
[15] H. Hippler and J. Troe, in *Bimolecular Collisions*, edited by M. N. R. Ashford and J. E. Bagott (Royal Society of Chemistry, London, 1989) p. 209.
[16] H. G. Löhmannsröben and K. Luther, Chem. Phys. Lett. **144**, 473 (1988).
[17] W. Jalenak, R. E. Weston, Jr., T. J. Sears, and G. W. Flynn, J. Chem. Phys. **89**, 2015 (1988).
[18] J. R. Barker and B. M. Toselli, Int. Rev. Phys. Chem. **12**, 305 (1990).
[19] M. J. Rossi, J. R. Pladziewicz, and J. R. Barker, J. Chem. Phys. **78**, 6695 (1983).
[20] J. D. Brenner, J. P. Erinjeri, and J. R. Barker, Chem. Phys. **175**, 99 (1993).
[21] B. M. Toselli and J. R. Barker, J. Chem. Phys. **97**, 1809 (1992).
[22] B. M. Toselli, J. D. Brenner, M. L. Yerram, W. E. Chin, K. D. King, and J. R. Barker, J. Chem. Phys. **95**, 176 (1991).
[23] A. Bolovinos, P. Tsekeris, J. Philis, E. Pantos, and G. J. Andritsopoulos, Mol. Spectrosc. **103**, 240 (1984).
[24] B. M. Toselli and J. R. Barker, J. Chem. Phys. **95**, 8108 (1991).
[25] J. R. Barker, J. Monat, L. A. Miller, and J. D. Brenner (in preparation).
[26] J. F. Durana and J. D. McDonald, J. Chem. Phys. **64**, 2518 (1977).
[27] J. R. Barker and R. E. Golden, J. Phys. Chem. **88**, 1012 (1984).
[28] J. R. Barker, J. Phys. Chem. **96**, 7361 (1992).
[29] J. R. Barker, J. D. Brenner, and B. M. Toselli, Adv. Chem. Kinetics Dyn. **2B**, 393 (1995).
[30] C. A. Michaels, H. C. Tapalian, Z. Lin, E. T. Sevy, and G. W. Flynn, Faraday Discuss. (in press); (private communication).
[31] H. Hippler, J. Troe, and H. J. Wendelken, J. Chem. Phys. **78**, 6709 (1983).
[32] K. B. Hewett, M. Shen, C. L. Brummel, and L. A. Philips, J. Chem. Phys. **100**, 4077 (1994).
[33] K. K. Innes, J. P. Byrne, and I. G. Ross, J. Mol. Spectrosc. **22**, 125 (1967).
[34] G. Z. Whitten and B. S. Rabinovitch, J. Chem. Phys. **38**, 2466 (1963).
[35] G. Z. Whitten and B. S. Rabinovitch, J. Phys. Chem. **41**, 1883 (1964).
[36] W. Forst, *Theory of Unimolecular Reactions* (Academic, New York, 1973).
[37] J. R. Barker, Chem. Phys. **77**, 301 (1983).
[38] J. R. Barker and K. D. King, J. Chem. Phys. **103**, 4953 (1995), and references therein.
[39] V. D. Knyazev, J. Phys. Chem. **99**, 14738 (1995).
[40] Y. Guo, D. L. Thompson, and T. D. Sewell, J. Chem. Phys. **104**, 576 (1996).

[41] Gilbert, R. G., Int. Rev. Phys. Chem. **10**, 319 (1991).
[42] B. M. Toselli and J. R. Barker, Chem. Phys. Lett. **174**, 304 (1990).
[43] K. F. Lim and R. G. Gilbert, J. Phys. Chem. **94**, 72 (1990); **94**, 77 (1990)
[44] K. F. Lim, J. Chem. Phys. **100**, 7385 (1994); **101**, 8756 (1994).
[45] V. Bernshtein and I. Oref, J. Chem. Phys. **104**, 1958 (1996).
[46] T. Lenzer and K. Luther, J. Chem. Phys. **104**, 3391 (1996).
[47] M. L. Yerram, J. D. Brenner, K. D. King, and J. R. Barker, J. Phys. Chem. **94**, 6341 (1990).